

Vibrational and Quantum-Chemical Study of Nonlinear Optical Chromophores Containing Dithienothiophene as the Electron Relay

Juan Casado,^[a] Víctor Hernández,^[a] Oh-Kil Kim,^[c] Jean-Marie Lehn,^[d]
 Juan T. López Navarrete,^{*[a]} Salvador Delgado Ledesma,^[a] Rocío Ponce Ortiz,^[a]
 Mari Carmen Ruiz Delgado,^[a] Yolanda Vida,^[b] and E. Pérez-Inestrosa^[b]

Dedicated to Professor Giuseppe Zerbi on the occasion of his 70th birthday in acknowledgement of his contributions to the field of vibrational spectroscopy of organic materials

Abstract: A series of nonlinear optical (NLO) donor–acceptor (D–A) chromophores containing a fused terthiophene, namely dithienothiophene (**DTT**), as the electron relay, the same donor group, and acceptors of various strengths, has been investigated by means of infrared and Raman spectroscopies, both in the solid state as well as in a variety of solvents, to evaluate the effectiveness of the intramolecular charge transfer from the electron-donor to the electron-acceptor end groups. The Raman spectral profiles of these NLO-phores measured from their dilute solutions have been found to be rather similar to those of the corresponding solids, and thus their intramolecular charge transfer (ICT) shows very little dependence on the solvent polarity. The experimental results obtained for the **DTT**-containing NLO-

phore with a 4-(*N,N*-dibutylamino)styryl end group as the donor and a 2,2-dicyanoethen-1-yl end group as the acceptor differ from those previously obtained for two parent “push–pull” chromophores with the same D–A pair but built-up around either a bis(3,4-ethylenedioxythienyl) (BEDOT) or a bithienyl (BT) electron relay. Vibrational spectroscopy shows that **DTT** is significantly more efficient as an electron relay than BT (which has the same number of conjugated C=C bonds) or BEDOT (which can be viewed as a rigidified version of BT on

account of noncovalent intramolecular interactions between heteroatoms of adjacent rings). Density functional theory (DFT) calculations have also been performed on these NLO-phores to assign their main electronic and vibrational features and to obtain information about their structures. An additional merit of these molecular materials was revealed by the infrared spectra of the **DTT**-based NLO-phores recorded at different temperatures. Thus, spectra recorded between –170 and 150 °C did not show any substantial change, indicating that the materials have a high thermal stability, which is of significance for their use as active components in optoelectronic devices.

Keywords: density functional calculations · IR spectroscopy · nonlinear optics · push–pull oligomers · Raman spectroscopy · vibrational spectroscopy

[a] Dr. J. Casado, Prof. Dr. V. Hernández,
 Prof. Dr. J. T. López Navarrete, Eng. S. Delgado Ledesma,
 Eng. R. Ponce Ortiz, Eng. M. C. Ruiz Delgado
 Departamento de Química Física, Facultad de Ciencias
 Universidad de Málaga, 29071 Málaga (Spain)
 Fax: (+34)952-132000
 E-mail: teodomiro@uma.es

[b] Y. Vida, Prof. Dr. E. Pérez-Inestrosa
 Departamento de Química Orgánica, Facultad de Ciencias
 Universidad de Málaga, 29071 Málaga (Spain)

[c] Dr. O.-K. Kim
 Chemistry Division, Naval Research Laboratory, Washington DC
 20375-5342 (USA)

[d] Prof. Dr. J.-M. Lehn
 Chimie des Interactions Moléculaires, Collège de France
 11 Place Marcellin Berthelot, 75005 Paris (France)

Introduction

The nonlinear optical (NLO) activity of push–pull chromophores is determined not only by the donor–acceptor (D–A) strengths of their end groups, but more subtly by conjugated electron relays. This is evident from the different relay activities observed for different π -conjugated relays, such as a polyene and an oligophenylene of the same chain length, bearing the same D–A pair; in a given solvent a larger red-shift of the low-energy absorption maximum, λ_{max} , is observed for polyenes than for oligophenylenes. Such a dispersion of the UV-visible absorption of the D–A chromophores becomes even more pronounced with increasing polarity of the solvent. This “positive solvatochromism” is regarded as

an indication of the molecular nonlinearity ($\mu\beta$) of the NLO chromophores.^[1–3]

Oligothiophenes are well recognized for their ability to act as relays, with efficiencies comparable to those of polyenes, which is ascribed to their lower resonance energy as compared to benzene. In fact, their conjugation effect could be even more pronounced than that of polyenes due to their rigid ring structures and the fact that adjacent units can adopt coplanar arrangements. Examination of the results from various studies on the relay efficiencies of oligothiophenes^[2] and oligophenylenes^[4,5] indicates that thiophene-based π -conjugated spacers make a more pronounced contribution to $\mu\beta(0)$ values than the oligophenylenes, and that whereas oligophenylenes attain a rapid saturation beyond a terphenyl unit, oligothiophenes show a strong tendency to increase $\mu\beta(0)$ with increasing number of thienyl units. In this regard, it is interesting to investigate the effectiveness of fused thiophenes as relays, since the rigidification of thienyl units (by cyclization) could favor π -conjugation and thus more effective charge-transfer in push–pull chromophores; this would be manifested in a bathochromic shift of the absorption bands and a strong solvatochromism compared to the corresponding flexible relays with the same number of units or π -electrons.^[6–8] A further fact that illustrates the effectiveness of fused thiophenes as relays is that their longest wavelength absorptions show an excellent linear correlation with the number of the thiophene rings, at least up to five units.^[9] Some of us have recently reported on the synthesis of D–A chromophores with a common donor group and acceptors of various strengths, containing a central π -conjugated dithieno[3,2-*b*:2',3'-*d*]thiophene (DTT) electron relay, and on their solvatochromism and molecular nonlinearity.^[10]

Vis-NIR electronic absorption and IR and Raman spectroscopic measurements have been successfully used as complementary techniques to study many different classes of π -conjugated polymers and oligomers, systems which show strong electron-phonon coupling due to their quasi one-dimensional structures. Raman spectroscopy has been shown to be a particularly powerful tool for: i) estimating the degree of π -conjugation in the neutral state,^[11–13] ii) characterizing different types of charged defects in doped π -conjugated materials,^[14] and iii) analyzing the intramolecular charge transfer in push–pull π -conjugated NLO-phores.^[15,16] On the basis of the assumptions of effective conjugation coordinate (ECC) theory,^[17] the appearance of only a few overwhelmingly strong Raman bands is attributed to the existence of an effective electron-phonon coupling over the whole π -conjugated backbone. As for aromatic and heteroaromatic polyconjugated systems, the ECC vibrational coordinate takes the analytical form of a linear combination of ring C=C/C–C stretchings, and allows a distinction to be made between a benzenoid-type structure (usually that of the ground state) and a quinonoid-type structure (that corresponding to the electronically excited state or the oxidized species). The ECC model states that as the conjugation length (CL) increases, the totally symmetric normal modes of the neutral system mostly involved in the molecular dynamics of the ECC coordinate (i.e., those which give rise to

the few Raman bands observed experimentally) undergo sizeable frequency and intensity dispersions. Thus, changes in peak positions and relative intensities of Raman features among a given series of π -conjugated oligomers of increasing chain length are quite useful in evaluating the effective CL for such a family of homologous oligomers. On the other hand, when a π -conjugated system, and particularly an oligothiophene system, becomes photoexcited or oxidized (either chemically or electrochemically), quinonoid-like conjugational defects are typically created.^[18] These structural changes produce a significant downshift of the Raman bands associated with the π -conjugated skeleton. The evolution of the Raman spectral profile between the neutral and the various doped states is a useful tool for elucidating the type and size of charge carriers created upon oxidative doping.^[11–14]

The results we present herein consist of FT-Raman, FT-IR, and UV/Vis/NIR electronic absorption spectroscopic measurements on three NLO-phores built up around a DTT relay, both in the solid state and in a variety of solvents, along with supporting quantum-chemical calculations. The Raman features are compared for solids and solutes, and for the NLO-phores and some donor-substituted (D–DTT) or acceptor-substituted (DTT–A) model compounds, to analyze the degree of intramolecular charge transfer (ICT) from the donor to the acceptor groups. The Raman-active $\nu(\text{CN})$ stretching vibrations of the NLO-phores containing a dicyanomethylene moiety as the electron acceptor are expected to be particularly diagnostic of the degree of ICT. Density functional theory (DFT) calculations have also been carried out for guidance in the analysis of the electronic and vibrational spectra and to derive relevant molecular parameters regarding bond lengths and atomic charge distributions. Thus, the various measurements and theoretical data described herein significantly enhance our understanding of the electronic and geometric structures of this type of D– π –A systems, a subject of considerable current interest.

Results and Discussion

Synthesis and UV/Vis absorption maxima: The chemical structures of the NLO-phores and some model systems studied in this work are depicted in Figure 1, along with the abbreviations used to denote them herein. The three push–pull chromophores bear a 4-(*N,N*-dibutylamino)styryl end group as the donor and an acceptor derived from formaldehyde (D₁–DTT–A₁), malonitrile (D₁–DTT–A₂), or *N,N*-diethylthiobarbituric acid (D₁–DTT–A₃). Their synthesis has been reported in detail elsewhere.^[10] An established procedure, specifically the Vilsmeier reaction, was used to convert DTT into its α -monoformyl derivative, DTT–A₁, in good yield (83%). Introduction of the 4-(*N,N*-dibutylamino)styryl electron-donor, yielding D₁–DTT, was achieved by Wittig olefination of the monoaldehyde DTT–A₁ by condensing it with 4-(*N,N*-dibutylaminobenzyl)triphenylphosphonium iodide in dichloromethane containing potassium *tert*-butoxide. The less soluble *E* isomer could be isolated in pure form from the semi-solid mixture of the *E* and *Z* isomers by precipita-

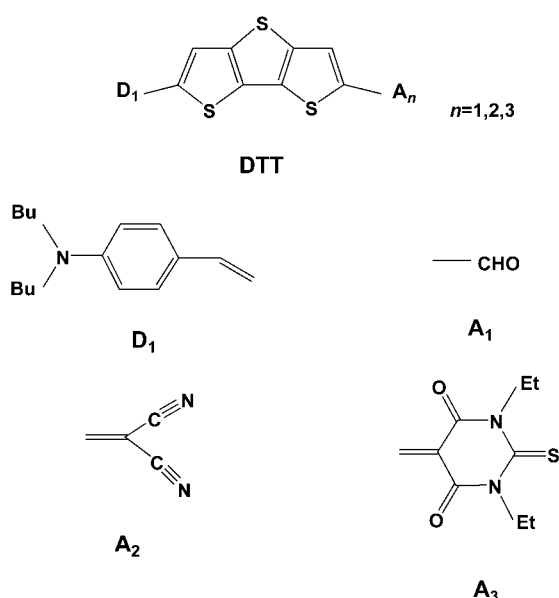


Figure 1. Chemical structures and associated abbreviations used throughout the text.

tion after washing with *n*-pentane. Alternatively, Knoevenagel condensation between malononitrile and **DTT-A₁** under acid-catalyzed (AcOH/NH₄OAc) conditions in toluene led to **DTT-A₂** in good yield (90 %).

Table 1 lists the UV/Vis absorption maxima, λ_{\max} , of the three push-pull chromophores in CH₂Cl₂ and DMF solutions, together with those of the unsubstituted **DTT** electron relay and the three model systems **D₁-DTT**, **DTT-A₁**, and **DTT-A₂**. As expected, the lowest energy absorption of the NLO-phores is increasingly red-shifted with increasing acceptor strength, reflecting the differences in the electronic transition associated with the ICT between the D and A groups. Among the three acceptors, **A₃** is the strongest, such that the electronic ground-state structure of **D₁-DTT-A₃** is, relatively speaking, the most polarized and that of **D₁-DTT-A₁** the least polarized. In other words, the contribution of the charge-separated form to the ground-state structure (see Figure 2) is greatest for **D₁-DTT-A₃** and smallest for **D₁-DTT-A₁**. The absorption data also show that in contrast to **D₁-DTT-A₁**, chromophores **D₁-DTT-A₂** and **D₁-DTT-A₃** exhibit solvatochromic behavior on going from CH₂Cl₂ to DMF that is at variance with the typical bathochromic shift or positive solvatochromism with increasing polarity of the solvent commonly observed for many classes

Table 1. UV/Vis absorption maxima (λ_{\max}) of the various compounds studied in this work, in CH₂Cl₂ and DMF solutions.

Compound	CH ₂ Cl ₂ ^[a]	DMF ^[a]
D₁-DTT-A₁	470	470
D₁-DTT-A₂	570	556
D₁-DTT-A₃	622	610
DTT	282, 290, 298	
D₁-DTT	408	410
DTT-A₁	354	354
DTT-A₂	432	432

[a] λ_{\max} values in nm.

of push-pull chromophores based on other electron relays. This phenomenon could be explained in terms of greater ground-state polarization for the latter two NLO-phores, meaning that in **D₁-DTT-A₂** and **D₁-DTT-A₃** there is a comparatively larger contribution of the zwitterionic form in the ground-state structure, whereas a predominance of the neutral form is to be expected in the ground state of **D₁-DTT-A₁**.

Optimized geometries and electronic spectra: Figure 2 shows, from a simple chemical point of view, the two limiting resonance forms that contribute with different weights to the description of the electronic structure of a push-pull

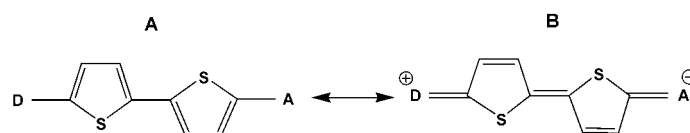


Figure 2. Neutral and charge-separated limiting resonance forms for the class of push-pull π -conjugated NLO-phores.

π -conjugated oligomer. In the neutral form, no ICT from the donor to the acceptor takes place, and the central spacer displays a fully aromatic structure. In the charge-separated form, however, one electron is fully transferred from the donor to the acceptor, and the π -conjugating spacer becomes fully quinoidized.

The main factors that determine the degree of polarization of the π -electron cloud of the spacer are: i) the strengths of the donor and acceptor end groups, ii) the chemical nature of the spacer (i.e., oligoene, oligothiophene, oligothiénylvinylene, etc.), and iii) the number of units in the π -conjugated chain. The first consequence of the existence of an efficient ICT in the push-pull oligomer is the appearance of a molecular dipole moment (generally large) directed from the acceptor to the donor, the magnitude of which is increased with increasing polarization of the molecule. A second consequence concerns the molecular geometry of the central spacer. At first glance, the actual electronic structure of a push-pull π -conjugated oligomer can be considered to result from a linear combination of the two limiting resonance forms plotted in Figure 2. The relative stability of the zwitterionic form with respect to the neutral form determines the weights of the contributions of these two canonical structures to the linear combination that describes the structure of the chromophore.

For a better understanding of the equilibrium molecular geometries and charge distributions of the three NLO-phores, we performed optimizations within the framework of DFT, based on B3LYP/6–31G** model chemistry. Figure 3 displays the main skeletal bond lengths for **D₁-DTT-A₁**, **D₁-DTT-A₂**, and **D₁-DTT-A₃** (those for **DTT**, **D₁-DTT**, **DTT-A₁**, and **DTT-A₂** are available upon request from the authors).

The theoretical data suggest that the conjugated C=C/C–C bonds of the acceptor subunit are mainly affected by the electronic interaction with the electron-withdrawing end

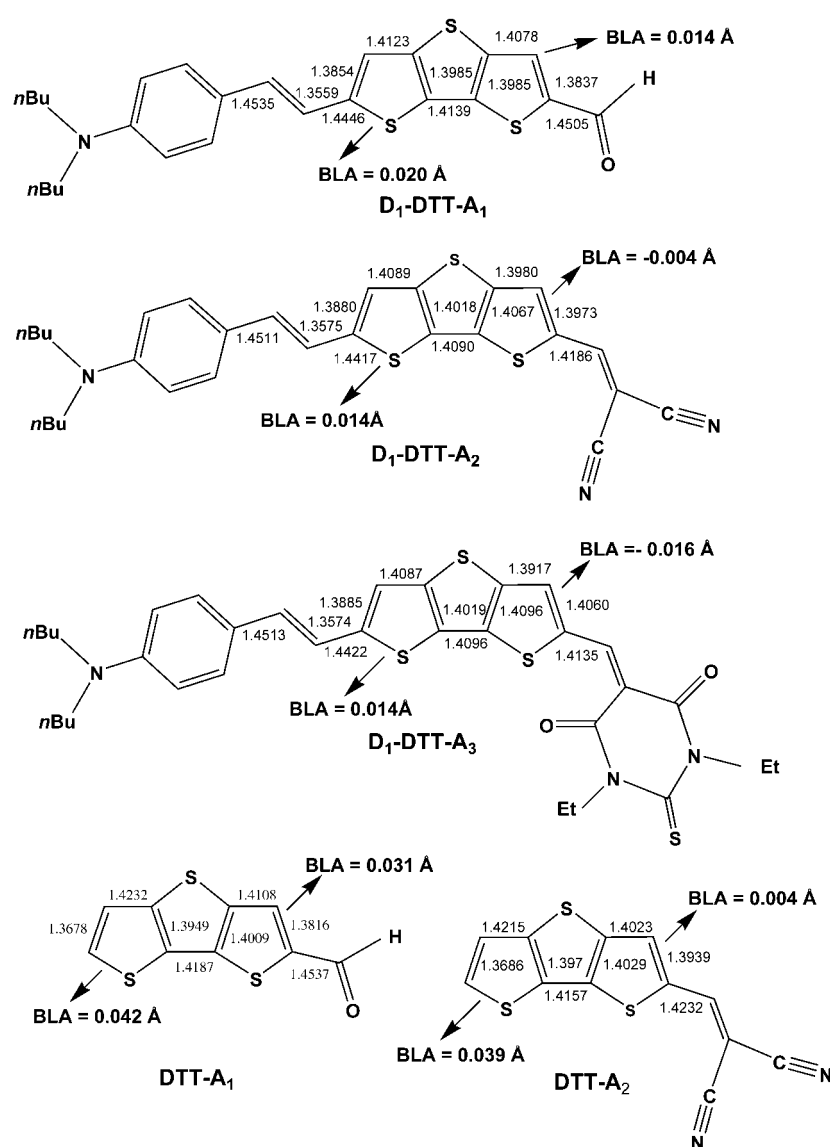


Figure 3. DFT//B3LYP/6-31 G** optimized skeletal bond lengths for **D₁-DTT-A₁**, **D₁-DTT-A₂**, **D₁-DTT-A₃**, **DTT-A₁**, and **DTT-A₂**.

group, whereas those of the donor subunit are less affected by the interaction with the electron-donating group. For **D₁-DTT-A₁**, the mean value of the successive single-double CC bond length alternation pattern (BLA) of the thienyl rings attached to the acceptor and to the donor amount to 0.014 and 0.020 Å, respectively, while the corresponding values for the other two NLO-phores are -0.004 and 0.014 Å (**D₁-DTT-A₂**) and -0.016 and 0.014 Å (**D₁-DTT-A₃**). These BLA values can be compared with the values computed for the other four systems: 0.045 Å (**DTT**), 0.042 and 0.026 Å (**D₁-DTT**), 0.031 and 0.042 Å (**DTT-A₁**), and 0.004 and 0.039 Å (**DTT-A₂**). Thus, the attachment of an acceptor group to the **DTT** relay induces a sizeable quinoidization of the acceptor-substituted thienyl ring (particularly for **DTT-A₂**, **D₁-DTT-A₂**, and **D₁-DTT-A₃**), although the geometrical modifications induced by the strong polarization of the π -electron cloud quickly decrease with distance from the acceptor end group. On the other hand, the attachment of the

4-(*N,N*-dibutylamino)styryl donor group to **DTT** gives rise to only moderate changes in the bond lengths and angles. We also observe that the C–S bond length varies significantly depending on the NLO-phore structure, mainly as a result of steric hindrance or electrostatic interactions with the substituents.

Contrary to the rather simplified general chemical description of the ground-state structure of a π -conjugated push-pull chromophore in terms of extreme Kekulé canonical forms such as those sketched in Figure 2 (i.e., with the neutral form displaying fully aromatic-like character over the whole π -conjugated path, and the zwitterionic form being characterized by a fully quinonoid-like reversed pattern), we observe that the DFT molecular geometry optimizations performed for these push-pull NLO-phores predict the coexistence of two different molecular domains within the π -conjugated spacer. This situation arises because of the stronger interaction of the **DTT** relay with the acceptor than with the donor, as a result of which the fused thienyl ring directly linked to the electron-withdrawing group displays a larger degree of quinoidization than that linked to the donor.

Figure 4 shows the natural bond orbital atomic charges on the donor and the acceptor end groups for the three NLO-phores, the whole π -conjugated electron relay, and each of the molecular domains hypothesized to lie within it. Each outermost thienyl unit of unsubstituted **DTT** is predicted to bear an overall charge of $-0.491 e$ (i.e., without taking into account the sum of the $0.264 e$ NBO atomic charges on each hydrogen at the end α -positions), which is balanced by an atomic charge of $0.454 e$ on the central sulfur bridging the two innermost β -positions of the electron relay (NBO atomic charges for **DTT**, **D₁-DTT**, **DTT-A₁**, and **DTT-A₂** are available upon request from the authors). DFT//B3LYP/6-31 G** model chemistry reveals an interesting difference with respect to the rather simple charge distribution associated with the zwitterionic canonical form plotted in Figure 2. Thus, the natural bond orbital atomic charges on the donor and acceptor groups amount to 0.106 and $-0.193 e$, respectively, for **D₁-DTT-A₂**, and to 0.102 and $-0.231 e$ in the case of the NLO-phore **D₁-**

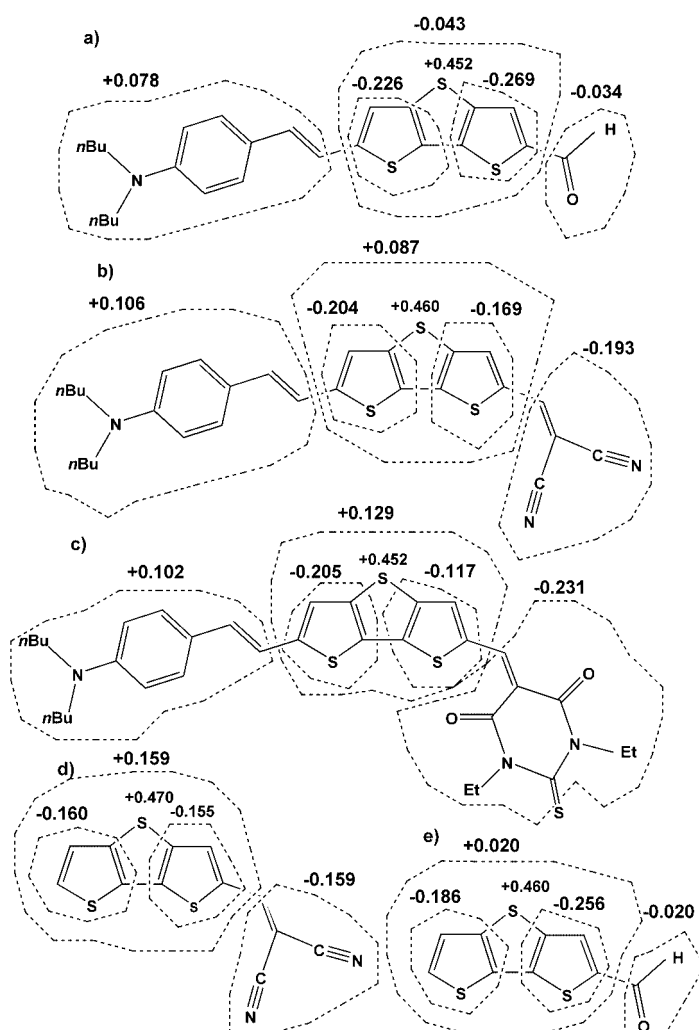


Figure 4. Natural bond orbital atomic charges for **D₁-DTT-A₁**, **D₁-DTT-A₂**, **D₁-DTT-A₃**, **DTT-A₁**, and **DTT-A₂** as deduced from their optimized DFT/B3LYP/6-31 G** molecular geometries.

DTT-A₃. Thus, B3LYP/6-31 G** calculations indicate that for these two push-pull systems the charge on the electron-withdrawing group is around twice that on the 4-(*N,N*-dibutylamino)styryl donor group, and that the π -conjugated electron relay is highly polarized since it bears up to 40–50% of the net positive charge of the whole NLO-phore (0.087 *e* for **D₁-DTT-A₂** and 0.129 *e* for **D₁-DTT-A₃**). By looking at the net charges on the outermost thienyl units of the spacer, we notice that the **DTT** subunits attached to the donor and the acceptor bear -0.204 and -0.169 *e*, respectively, in the case of **D₁-DTT-A₂**, and -0.205 and -0.117 *e* in the case of **D₁-DTT-A₃**. These net charges can be compared with the aforementioned value of -0.491 *e* obtained for each thienyl ring of **DTT**, indicating that the electron relay interacts more strongly with the acceptor than with the donor. Finally, we also note that the central sulfur atom plays a minor role in the ICT since its NBO atomic charge amounts to 0.453 *e* for **DTT**, 0.452 *e* for **D₁-DTT-A₁**, 0.460 *e* for **D₁-DTT-A₂**, and 0.452 *e* for **D₁-DTT-A₃**.

To rationalize the evolution of the electronic absorption properties in the push-pull materials, the electronic spectra

of the three NLO-phores were calculated at the B3LYP/6-31 G** level within the framework of the time-dependent DFT (TDDFT) approach. TDDFT calculations predict one intense electronic transition at 2.58 eV (with oscillator strength $f = 1.29$), 2.16 eV ($f = 1.28$), and 2.10 eV ($f = 1.51$) for **D₁-DTT-A₁**, **D₁-DTT-A₂**, and **D₁-DTT-A₃**, respectively, in good accordance with the experimental data. In all the cases, this electronic absorption corresponds to the transition from the ground to the first excited state and is mainly described by one-electron excitation from the highest occupied molecular orbital (HOMO) to the lowest unoccupied molecular orbital (LUMO). The intense absorption observed at 470 nm (2.64 eV) for **D₁-DTT-A₁**, at 570 nm (2.18 eV) for **D₁-DTT-A₂**, and at 622 nm (1.99 eV) for **D₁-DTT-A₃** is therefore assigned to the HOMO \rightarrow LUMO one-electron promotion calculated to lie at around 2.2 eV.

The atomic orbital compositions of the frontier molecular orbitals are sketched in Figure 5. For the three NLO-phores

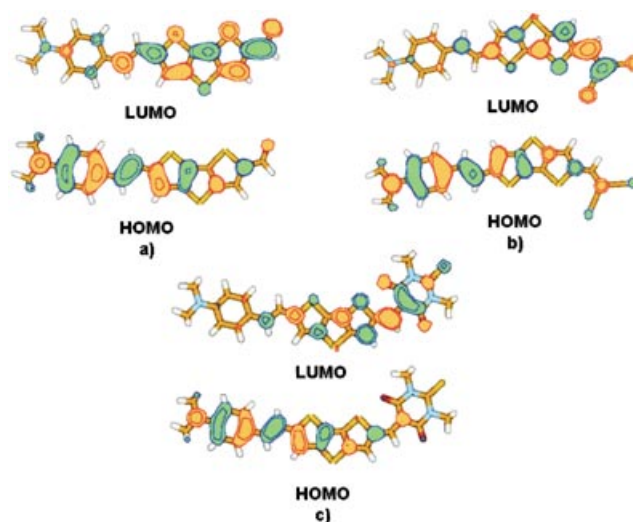


Figure 5. Electronic density contours ($0.03 e_{\text{bohr}}^{-3}$), calculated at the B3LYP/6-31 G** level, for the HOMO and LUMO frontier molecular orbitals of **D₁-DTT-A₁**, **D₁-DTT-A₂**, and **D₁-DTT-A₃**.

studied in this work, the HOMO is of π nature and is delocalized along the CC backbone (with a small contribution from the thienyl unit linked to the acceptor group) and on the 4-(*N,N*-dibutylamino)styryl electron-donor group. In contrast, the LUMO in these three chromophores is concentrated on the acceptor and extends to the **DTT** electron relay. This is also the case for the three monosubstituted model systems: the HOMO topology in **D₁-DTT** greatly resembles those of the HOMOs in the push-pull NLO-phores, whereas the LUMOs in **DTT-A₁** and **DTT-A₂** are similar to those of **D₁-DTT-A₁** and **D₁-DTT-A₂**, respectively. Consequently, the HOMO \rightarrow LUMO transition in the NLO-phores implies an electron density transfer from the more aromatic domain of the π -conjugating spacer, including the electron-donor group, to its more quinonoid side and to the electron-withdrawing group. The topology of the frontier molecular orbitals thus demonstrates the charge-transfer character of the HOMO \rightarrow LUMO transition, and also

shows the HOMO–LUMO overlap in the middle of the **DTT** electron relay, which is a prerequisite for facilitation of the charge-transfer transition and, consequently, for increasing the nonlinear optical response.

The attachment of an acceptor group to the **DTT** backbone has important consequences, not only for the atomic orbital compositions, but also for the energies of the frontier molecular orbitals. In Figure 6, it can be observed that the

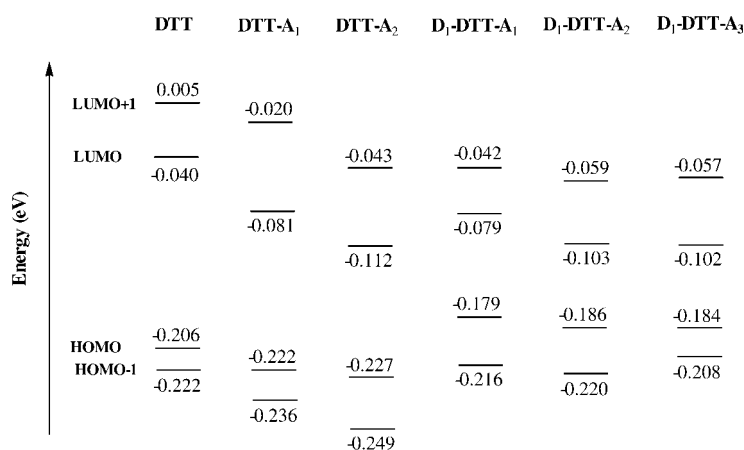


Figure 6. B3LYP/6-31 G** one-electron energies (ϵ_i) diagram showing the highest occupied and the lowest unoccupied molecular orbitals for all the molecules studied in this work.

attachment of an electron-withdrawing group, -CHO or -CH=C(CN)₂, to the **DTT** relay stabilizes both the HOMO and LUMO, by 0.016 and 0.041 eV, respectively, in the case of **DTT-A₁** and by 0.021 and 0.071 eV for **DTT-A₂**. In other words, the substitution of the end α -positions of the **DTT** relay with an electron-acceptor group lowers the relative energies of both the HOMO and LUMO, affecting the LUMO more than the HOMO, thus narrowing the HOMO–LUMO gap with respect to the unsubstituted π -conjugated system (i.e., this bandgap lowering is more pronounced the stronger the acceptor ability of the substituent). Upon monosubstitution of **DTT** with a 4-(*N,N*-dibutylamino)styryl donor group, both the HOMO and LUMO increase in energy, by 0.037 and 0.014 eV, respectively, thus giving rise to a slight bandgap narrowing. Finally, substitution of the two end α -positions of **DTT** with donor and acceptor end groups stabilizes the LUMO (by 0.039 eV in **D₁-DTT-A₁**, 0.063 eV in **D₁-DTT-A₂**, and 0.062 eV in **D₁-DTT-A₃**) and concomitantly destabilizes the HOMO (by 0.027 eV in **D₁-DTT-A₁**, 0.020 eV in **D₁-DTT-A₂**, and 0.022 eV in **D₁-DTT-A₃**), leading to an overall larger bandgap reduction than in the compounds **D₁-DTT**, **DTT-A₁**, and **DTT-A₂** (see Figure 6).

Experimental and theoretical IR and Raman spectra: In Figure 7, the IR and Raman spectral profiles of **D₁-DTT-A₂**, as a prototypical example of a push–pull chromophore, are compared with those of unsubstituted **DTT**, representing a nonpolar π -conjugated material. Some vibrational spectroscopic observations of general validity, which differentiate

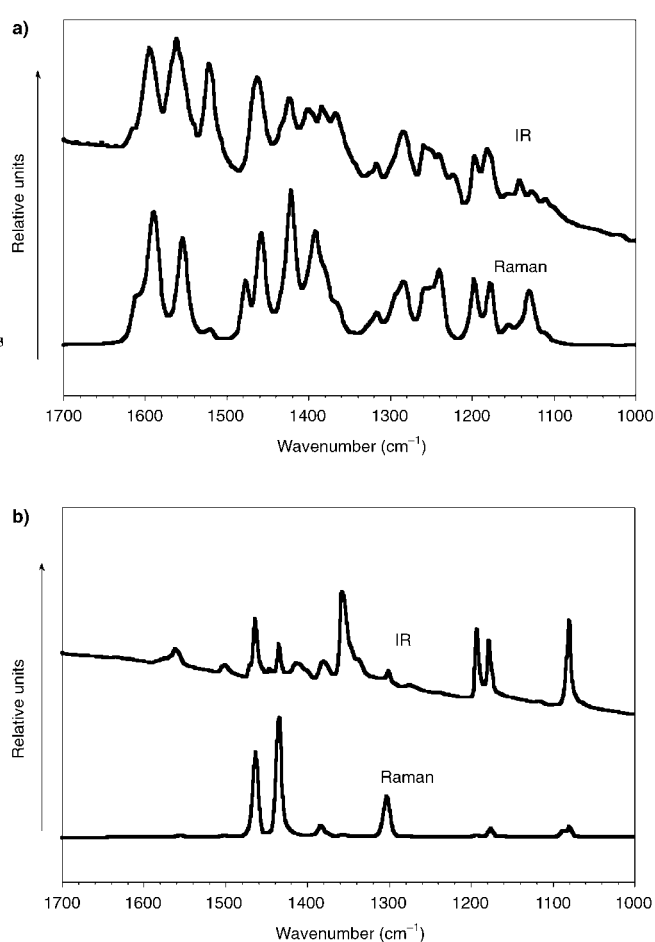


Figure 7. Comparisons of the IR and Raman spectra of: a) **D₁-DTT-A₂** as the prototypical example of a push–pull molecular material, and b) unsubstituted **DTT** as the prototypical example of the class of nonpolar π -conjugated materials.

the two classes of π -conjugated systems (i.e., push–pull and nonpolar), can be summarized as follows:

- 1) As mentioned in the introduction, the Raman spectra of the nonpolar π -conjugated oligomers are surprisingly simple. Only three or four overwhelmingly intense lines are observed in the 1600–1000 cm⁻¹ region, attributable to specific symmetrical skeletal C–C vibrations. This is due to strong electron-phonon coupling, which occurs in these systems due to their quasi one-dimensional structures (see the FT-Raman spectrum of **DTT** in Figure 7).^[11–17]
- 2) On the contrary, more than three or four strong scatterings are observed in the Raman spectra of the push–pull chromophores due to their low molecular symmetry. In general, the additional lines arise from vibrational coupling of the π -conjugating electron relay with stretching vibrations of the end groups (compare the FT-IR and FT-Raman spectra of **D₁-DTT-A₂** in Figure 7).^[15,16] The large molecular dipole moment directed from the acceptor to the donor imparts those vibrational normal modes of the π -conjugated backbone giving rise to the experimentally observed Raman bands with an extra-

large IR activity, due to the sizeable fluxes of charge induced along the strongly polarized alternating sequence of double/single C–C bonds. This is not the situation for the centrosymmetric nonpolar oligothiophenes; in these, the mutual exclusion principle holds due to the existence of an inversion center in the middle of the molecule, as a result of which Raman-active vibrations become almost undetectable in the IR spectrum, and vice versa. Furthermore, the out-of-plane $\gamma(\text{C–H})$ bending vibrations, appearing near 800 cm^{-1} , are usually by far the strongest infrared absorptions for the nonpolar oligothiophenes (see the FT-IR spectrum of **DTT** in Figure 7). Thus, for the push–pull materials, the resemblance between the IR and Raman spectral profiles can be considered as proof that an effective ICT takes place.^[15–16]

Let us now consider the vibrational spectroscopic analysis of the compounds studied in this work. Figure 8 shows the IR and Raman spectra of **DTT–A₁** and **DTT–A₂**, while those of the π -conjugated **DTT** moiety are depicted in Figure 7. The Raman spectrum of **DTT** displays three strong scatterings at 1464 , 1436 , and 1303 cm^{-1} ; of these, the former arises from a totally asymmetric $\nu_{\text{asymm}}(\text{C=C})$ stretch-

ing mode of the outermost thienyl units and is related to the commonly termed “*line A*” in α -linked oligothiophenes,^[11–13] while the second is due to a *collective oscillation of the whole alternating sequence of C=C/C–C bonds*, during which all π -conjugated C=C bonds lengthen in-phase while all π -conjugated C–C bonds shrink in-phase, which is denoted as the “*ECC mode*” or “*line B*” for linear oligothiophenes^[11–13] (the corresponding eigenvectors are plotted in Figure 9).

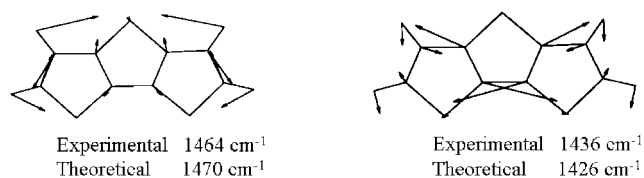


Figure 9. Schematic B3LYP/6-31 G** atomic vibrational displacements associated with the two strongest Raman lines of **DTT** experimentally measured at 1464 and 1436 cm^{-1} (quoted frequency values correspond to the theoretical ones scaled down by a factor of 0.96).

The *collective skeletal mode*, which gives rise to the strong Raman *line B*, mimics the change of the nuclear configuration of the π -conjugated system on going from a *heteroaromatic-like* pattern to a *heteroquinonoid-like* one, and its frequency allows analysis of the “softening” of the π -conjugated backbone, along a bunch of related NLO-phores, induced by the ICT.^[15,16]

Figure 8 shows the IR and Raman spectral profiles of **DTT–A₁** and **DTT–A₂**. The strong IR and Raman features of **DTT–A₁** at 1650 cm^{-1} , due to the aldehyde $\nu(\text{C=O})$ stretching, are no longer seen after replacing the **A₁** acceptor by the dicyanoethylene group **A₂**. On the other hand, new IR and Raman bands measured for **DTT–A₂** at 2218 and 1570 cm^{-1} can be attributed to the $\nu(\text{C}\equiv\text{N})$ stretchings and the vinylic $\nu(\text{C=C})$ stretching, respectively, of the $\text{C}(\text{CN})_2$ moiety connected to the **DTT**. In full accordance with the predictions of the ECC model, we also observe that the peak position of the strongest Raman *line B*, measured at 1436 cm^{-1} for **DTT**, is red-shifted as the π -conjugated path is extended, appearing at 1429 cm^{-1} for **DTT–A₁** and at 1431 cm^{-1} for **DTT–A₂**, as a consequence of the “softening” of the molecular backbone caused by the attachment of the acceptor to the **DTT** spine. On the other hand, *line B* appears at nearly the same position for **D₁–DTT** (1435 cm^{-1}) and unsubstituted **DTT** (1436 cm^{-1}), indicating that the attachment of a single 4-(*N,N*-dibutylamino)styryl donor group does not significantly improve the overall π -conjugation.

The Raman spectra of the various NLO-phores (obtained in the form of pure powders) are compared with the corresponding B3LYP/6-31 G** model spectra in Figure 10. The agreement between theory and experiment is remarkably satisfactory for all the compounds. Nonetheless, a complete assignment of the IR and Raman bands of each NLO-phore to particular vibrations is beyond the scope of our analysis. We will restrict our discussion only to the most relevant observations.

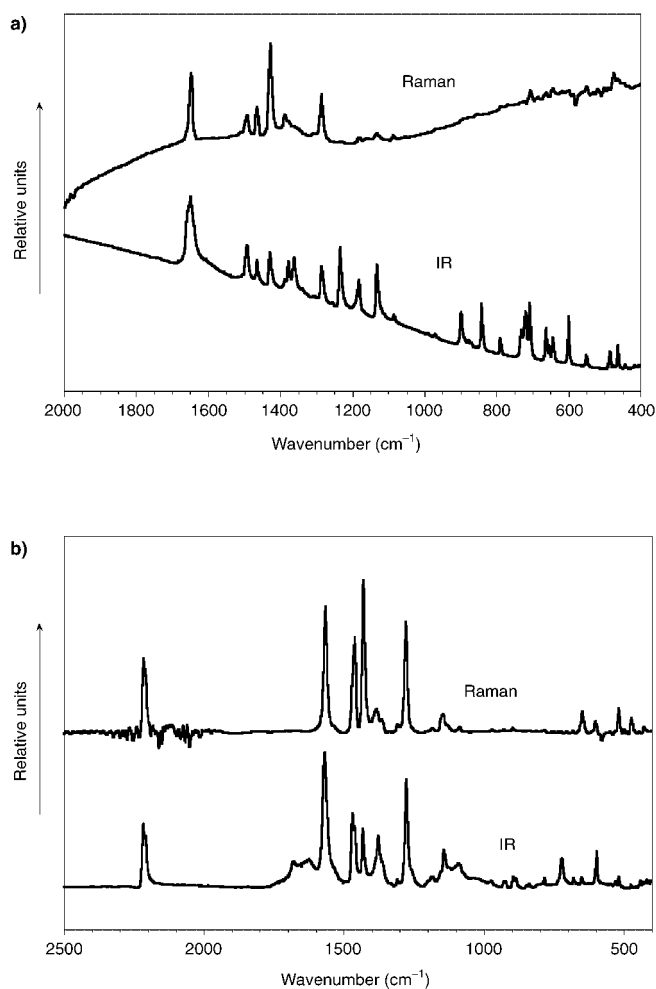


Figure 8. IR and Raman spectral profiles of: a) **DTT–A₁** and b) **DTT–A₂**.

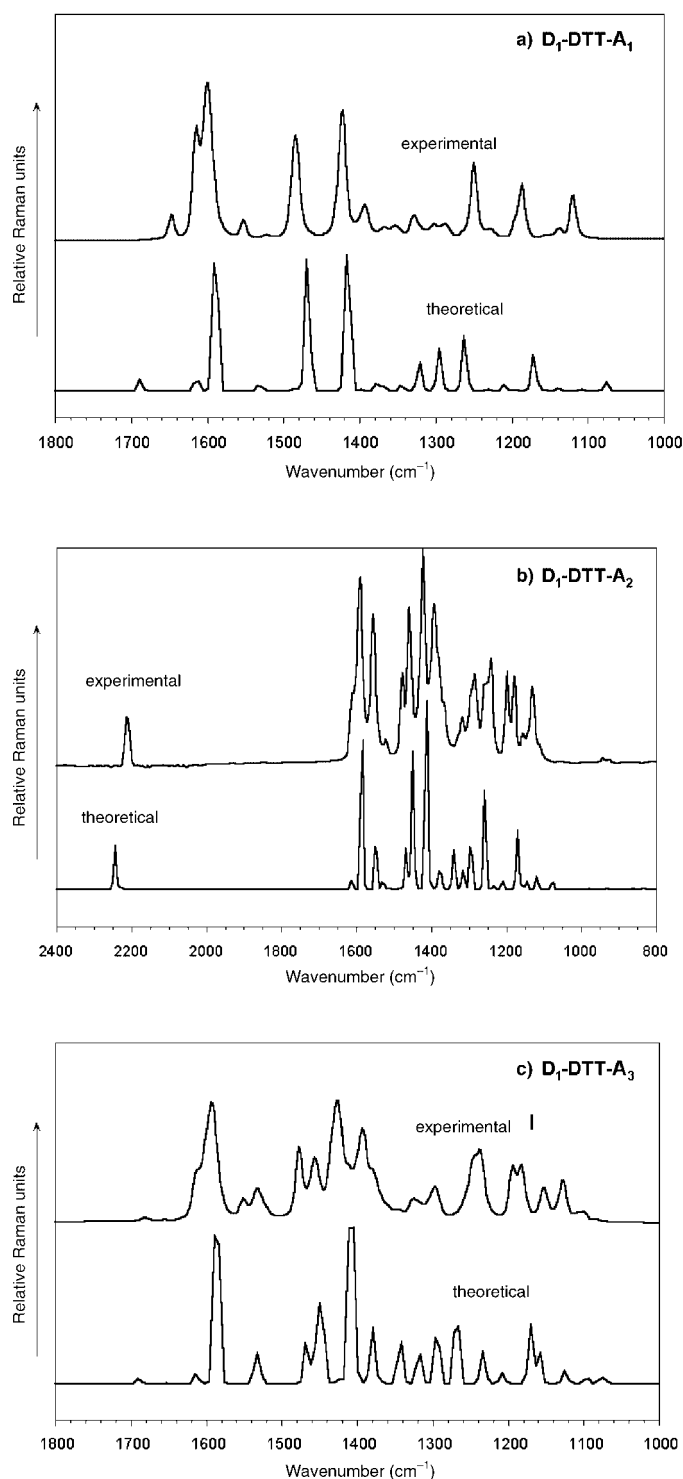


Figure 10. Comparison between the experimental and DFT//B3LYP/6-31 G** theoretical Raman spectra of a) $\mathbf{D}_1\text{-DTT-A}_1$, b) $\mathbf{D}_1\text{-DTT-A}_2$, and c) $\mathbf{D}_1\text{-DTT-A}_3$.

The strong Raman line at 1600 cm^{-1} ($\mathbf{D}_1\text{-DTT-A}_1$), 1590 cm^{-1} ($\mathbf{D}_1\text{-DTT-A}_2$), and 1592 cm^{-1} ($\mathbf{D}_1\text{-DTT-A}_3$) is due to a $\nu(\text{C}=\text{C})_{\text{ring}}$ stretching of the 4-*N,N*-dibutylaniline group extensively mixed with the $\nu(\text{C}=\text{C})$ stretching of the vinylenic bond between the donor and the **DTT** relay. The high intensity of this Raman scattering proves the sizeable

contribution of the 4-*(N,N)*-dibutylamino)styryl group to the ICT, while its $8\text{--}10\text{ cm}^{-1}$ red-shift on going from $\mathbf{D}_1\text{-DTT-A}_1$ to $\mathbf{D}_1\text{-DTT-A}_2$ and $\mathbf{D}_1\text{-DTT-A}_3$ is due to the increasing acceptor strengths of the \mathbf{A}_2 and \mathbf{A}_3 substituents.

The B3LYP/6-31 G** eigenvectors reveal that the strong Raman lines measured at 1422 cm^{-1} for $\mathbf{D}_1\text{-DTT-A}_1$, 1422 cm^{-1} for $\mathbf{D}_1\text{-DTT-A}_2$, and 1426 cm^{-1} for $\mathbf{D}_1\text{-DTT-A}_3$ (computed at 1415 , 1413 , and 1408 cm^{-1} , respectively) arise from the same *collective* $\nu(\text{C}=\text{C})$ stretching vibration that gives rise to *line B*. The red-shift of the “ECC mode” upon attaching the electron-donating 4-*(N,N)*-dibutylamino)styryl group and the electron-withdrawing end groups of various strengths (i.e., aldehyde, dicyanovinylene, and thiobarbituric acid) to the **DTT** relay is in full agreement with the predictions of the ECC model,^[17] and with what is found experimentally for neutral and doped oligothiophenes.^[13,14] Thus, for the neutral (non-polar) forms of a homologous series of α,α' -dimethyl end-capped oligothiophenes, the strongest Raman scattering was found at around 1480 cm^{-1} (a characteristic Raman marker of a *heteroaromatic*-like pattern of the π -conjugated backbone), and upon oxidation of the oligomers this was markedly down-shifted and split into two components at around 1440 and 1420 cm^{-1} (typical markers of the attainment of a *heteroquinonoid*-like pattern of the π -conjugated path). The relative intensities of these two doping-induced Raman scatterings depend on the degree of quinoidization of the π -conjugated backbone: that near 1440 cm^{-1} is stronger for the radical cationic species (for which the quinoidization mainly affects the inner units of the oligomer),^[14a] while that near 1420 cm^{-1} becomes stronger for the dicationic species (for which the quinoidization nearly extends over the whole chain due to the repulsion between the two positive charges).^[14b] Such a simple Raman spectral profile has also been found for a novel class of oligothiophenes bearing a pure heteroquinonoid structure in their electronic ground states.^[13e,14g] The softening of the ECC mode for the three NLO-phores by around 12 cm^{-1} with respect to its peak position in unsubstituted **DTT** is consistent with the net BLA value calculated for each fused-oligothienyl spacer as a whole: 0.0442 (**DTT**), 0.0186 ($\mathbf{D}_1\text{-DTT-A}_1$), 0.0069 ($\mathbf{D}_1\text{-DTT-A}_2$), and 0.0032 \AA ($\mathbf{D}_1\text{-DTT-A}_3$), indicative of the sizeable degree of quinoidization in the push-pull chromophores.

We also observe that *line B* appears at a lower frequency in $\mathbf{D}_1\text{-DTT-A}_2$ (1422 cm^{-1}) than in a parent NLO-phore bearing the same D-A pair but attached to a bithienyl spacer (1428 cm^{-1}).^[16a] Recall that the second NLO-phore displays an *anti*-arrangement of the two thienyl units (i.e., a coplanar structure favoring overlap between the $2p_z$ orbitals of the C atoms at the innermost α -positions of the electron relay, thus allowing for a more effective ICT). On the contrary, the outermost thienyl units in $\mathbf{D}_1\text{-DTT-A}_2$ display a *syn*-configuration, which is less favorable for π -conjugation, and thus it follows that the bridging of the innermost β -positions by a sulfur atom leads to a significant improvement in the properties of the relay as compared to the case of bithienyl, as shown by the more pronounced softening of the π -conjugated backbone upon attachment of the same D-A pair.

The large involvement of the two nitrile groups of the A_2 acceptor group in the overall ICT is clearly evidenced by the sizeable displacement towards lower frequencies, by around 50 cm^{-1} , of the Raman-active $\nu(\text{CN})$ stretching vibrations of $D_1\text{-DTT-A}_2$ (2211 cm^{-1}) and $DTT\text{-A}_2$ (2217 cm^{-1}), as compared with the value of 2265 cm^{-1} measured for a nonconjugated dicyanomethane model system (see Figure 11).

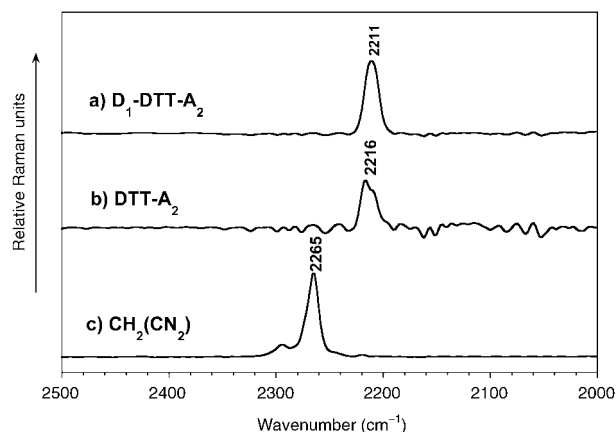


Figure 11. Raman bands due to the $\nu(\text{CN})$ stretching modes of a) $D_1\text{-DTT-A}_2$, b) $DTT\text{-A}_2$, and c) $\text{CH}_2(\text{CN})_2$ as pure solid samples.

IR and Raman spectra of the NLO-phores as solutes in dilute solutions: Figure 12 shows a comparison of the Raman spectra of $D_1\text{-DTT-A}_1$ obtained from a pure solid sample and from dilute solutions in CH_2Cl_2 and DMF (after subtracting the Raman scatterings of the corresponding solvent as appropriate). It can be noted that the vibrational spectral fingerprints of the two solutes are nearly superimposable on that recorded for the solid. In this regard, the main differences in peak positions of the Raman features do not exceed a 6 cm^{-1} blue-shift (see Table 2). It can also be noted that the relative intensities of the most prominent features remain almost unaffected in the three different environments. These spectroscopic data reveal that there is not a substantial loss of ICT for these DTT -containing chromophores on going from solids to solution. Nonetheless, the polar donor and acceptor end groups are expected to under-

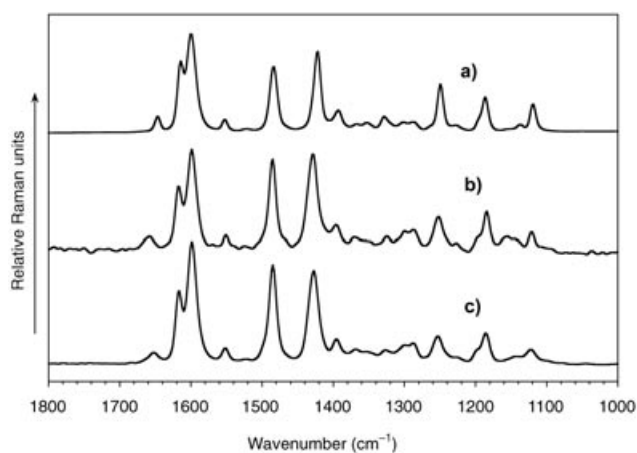


Figure 12. Raman spectral profiles of $D_1\text{-DTT-A}_1$ a) as a pure solid sample, b) in dilute CH_2Cl_2 solution, and c) in dilute DMF solution.

Table 2. Comparison between the frequencies (in cm^{-1}) of the Raman bands measured for $D_1\text{-DTT-A}_1$ in the solid state and in dilute CH_2Cl_2 and DMF solutions in the $1700\text{--}1000\text{ cm}^{-1}$ range.

Solid-state	Dilute CH_2Cl_2 solution	Dilute DMF solution
1647	1658	1653
1614	1617	1617
1600	1599	1599
1553	1551	1552
1522	1525	1522
1484	1485	1485
1422	1429	1428
1393	1396	1396
1367	1371	1369
1353	1356	1354
1329	1325	1327
1302	1300	1299
1288	1287	1288
1250	1252	1253
1228	1227	1227
1187	1185	1186
1137	1146	1142
1119	1121	1122

go some conformational distortions upon dissolution due to interactions with the solvents.

The Raman analysis of $D_1\text{-DTT-A}_2$ in solution (the results for which are similar to those reported above for $D_1\text{-DTT-A}_1$) is, however, in contrast to previous findings for two related push-pull chromophores with the same D-A pair but bearing either a bis(3,4-ethylenedioxythienyl) (BEDOT) or a bithienyl (BT) π -conjugated spacer instead of the DTT electron relay.^[16a] In that previous study, we observed that all Raman-active vibrations appearing between 1700 and 1250 cm^{-1} , among them those strongly related to the π -conjugated path, underwent a sizeable blue-shift (in some cases by more than 25 cm^{-1}) upon removing the solid-state packing forces and when solute-solvent interactions came into play (spectral differences were particularly significant for the BT-containing NLO-phore, due to the lack of rigidifying noncovalent $\text{S}\cdots\text{O}$ intramolecular interactions that exist between the adjacent rings of the BEDOT spacer). Following the same reasoning as in the above section on the Raman analysis of the NLO-phores as solids, the large up-shifts of the skeletal Raman vibrations upon dissolution observed for the BT- and BEDOT-containing chromophores were ascribed to a partial loss of overall π -conjugation of the system due to sizeable conformational distortions from coplanarity, not only of the electron-donating and electron-withdrawing end groups (as occurs for $D_1\text{-DTT-A}_1$, $D_1\text{-DTT-A}_2$, and $D_1\text{-DTT-A}_3$), but also of the two thienyl or EDOT subunits of the π -conjugated spacer.^[16a]

In conclusion, comparison of the Raman data obtained for the three DTT -containing NLO-phores studied here as solutes and as pure solids shows that their degree of ICT is almost unaffected by the solvent polarity. This must be ascribed not only to their rigid structures and to the effectiveness of DTT as an electron relay, but also to the large ground-state polarization through zwitterionic contributions.

Evolution of the FT-IR spectra with temperature: Figure 13 displays the evolution of the FT-IR spectrum of $D_1\text{-DTT-}$

A₁ with increasing temperature from -170°C to 150°C (103 K to 423 K); intermediate points at 90°C , 0°C , -60°C , -100°C , and room temperature ($\approx 20^{\circ}\text{C}$) were also analyzed.

The selected spectra shown in Figure 13 exhibit rather systematic trends, which are common to all the NLO-phores studied. No drastic spectral changes are seen for any of the

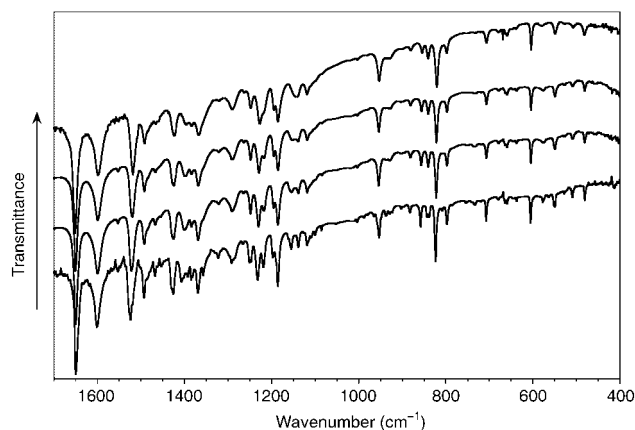


Figure 13. FT-IR spectra of **D**₁-**DTT**-**A**₁ measured at various temperatures; from bottom to top: -170°C , 0°C , RT, 150°C .

compounds before the maximum temperature is reached, and the FT-IR spectra reversibly recover their profiles throughout the whole temperature range examined. We also observe that at low temperatures the widths of the infrared bands neither substantially narrow nor split into well-resolved components, as would be expected for highly crystalline systems.

An opposite spectroscopic/thermal behavior was previously found for the series of crystalline α,α' -dimethyl end-capped oligothiophenes: i) the infrared absorptions of the dimer and trimer became substantially broader in the proximity of their respective melting points due to crystal disorder and subsequent loss of molecular symmetry in the melt caused by the rotations of the thiophene rings around the different inter-ring C–C bonds; ii) at low temperatures, some of the infrared bands were clearly resolved into sharp peaks due to the hindered internal rotation and the well-ordered intermolecular interactions induced by the close molecular packing.^[20]

Finally, the thermo-spectroscopic infrared absorption study of these **DTT**-containing NLO-phores indicates that, at least at the molecular scale, they could be used as active components for nonlinear optical (NLO) devices, which must be thermally stable at continuous working temperatures of about 80°C .^[21,22]

Summary and Conclusions

In summary, we have described the synthesis of some π -conjugated molecular materials containing a dithieno[3,2-*b*:2',3'-*d*]thiophene backbone with either an electron-donating 4-(*N,N*-dibutylamino)styryl group or an electron-withdrawing carbaldehyde or 2,2-dicyanoethen-1-yl group covalently attached to one of its end α -positions. These materials com-

plete a previously reported series of push–pull chromophores built around a rigid **DTT** (i.e., fused terthienyl) electron relay and bearing the same donor and acceptors of various strengths. Molecular geometry optimizations performed at the DFT//B3LYP/6-31G** level reveal an interesting result, which is in contrast with the classical view of push–pull molecules of this type in terms of resonance structures: the thienyl ring linked to the electron acceptor displays a partial quinonoid-like structure, while that directly connected to the electron donor retains a partial aromatic-like structure. Moreover, the equilibrium charge distributions derived from natural bond order (NBO) analysis of their optimized DFT//B3LYP/6-31G** molecular geometries indicate that the net negative charge on the acceptor is around twice as high as the positive charge on the 4-(*N,N*-dibutylamino)-styryl donor, that the **DTT** electron relay is highly and asymmetrically polarized since it bears nearly 40–50% of the net positive charge of the whole NLO-phore, and that the charge on the **DTT** subunit attached to the donor is always higher than that on the **DTT** subunit attached to the acceptor. The theoretical electrostatic picture of these NLO-phores also reveals that the central sulfur atom connecting the innermost β -positions of the fused terthienyl spine plays a minor role in the intramolecular charge transfer between the D/A end groups since it bears nearly the same NBO atomic charge in all of the compounds.

The three D- π -A systems studied in this work show an intramolecular charge-transfer band in the 450–600 nm spectral region, which is essentially unaffected by the solvent polarity. The topologies and relative energies of the molecular orbitals have been studied by means of TDDFT//B3LYP/6-31G** calculations, which revealed that the HOMO–LUMO energy gaps account for the observed ICT electronic absorptions, from the donor group, including its nearest thienyl ring, to the acceptor and the thienyl unit to which it is linked.

The compounds have also been analyzed by means of IR and Raman spectroscopies in the solid state as well as in dilute solutions. As a first result, the close resemblance between the IR and Raman spectral profiles of the D- π -A systems constitutes proof of a very effective intramolecular charge transfer. The π -conjugated **DTT** spacer gives rise to some characteristic collective vibrational normal modes (usually termed *ECC modes* in effective conjugation coordinate theory),^[17] during which changes in the molecular polarizability are quite significant. In the case of push–pull molecules, these Raman-active normal modes are also seen with high intensity in the IR spectra because of the significant polarization of the π -conjugated backbone due to the presence of polar D/A end groups. The high intensities of these IR-active vibrations can be attributed to the large fluxes of charge along the alternating sequence of C=C/C–C bonds during the *collective ECC skeletal oscillations*, which give rise to very large molecular dipole moment variations directed along the chain axis. The Raman spectroscopic data demonstrate that the rigidification of the innermost β -positions of the **DTT** electron relay through covalent bonds with a central sulfur atom improves the effectiveness of the intramolecular charge transfer with respect to related chromo-

phores built up around either bis(3,4-ethylenedioxythienyl) (BEDOT) or bithienyl (BT) spacers and bearing similar end D/A pairs.

Only very subtle differences in the Raman spectra of these DTT-containing NLO-phores as solutes and as pure solids were noted, which can be taken as an indication that the strong π -conjugation renders conformational distortions from coplanarity upon dissolution almost negligible. Finally, the FT-IR spectral profiles of the D- π -A systems recorded for solid samples at various intermediate temperatures between -170 and 150°C did not show any substantial changes. This indicates that, at least on the molecular scale, the materials have good thermal stability, which is of significance for their use as active components in practical optoelectronic devices.

Experimental and Theoretical Details

^1H and ^{13}C NMR spectra were recorded from samples in CDCl_3 solution on a Bruker WP-200 SY spectrometer operating at 200 and 50 MHz, respectively, using the solvent residual signal as a reference standard. EI mass spectra were recorded on a Hewlett Packard 5988 A mass spectrometer operating at 70 eV. UV/VIS/NIR absorption spectra were recorded on a Perkin-Elmer Lambda 19 spectrometer.

Fourier transform infrared absorption (FT-IR) spectra were recorded on a Bruker Equinox 55 spectrometer. Compounds were ground to a powder and pressed into KBr pellets. Spectra were collected with a spectral resolution of 2 cm^{-1} , and the mean of 50 scans was obtained. Interference from atmospheric water vapor and CO_2 was minimized by purging the instrument with dry argon prior to the data collection. FT-Raman spectra were collected in a back-scattering configuration on a Bruker FRA106/S apparatus coupled to an Nd:YAG laser source ($\lambda_{\text{exc}} = 1064\text{ nm}$). The operating power for the exciting laser radiation was kept to 100 mW in all the experiments. Samples were analyzed in the form of pure solids in sealed capillaries as well as in dilute CH_2Cl_2 and DMF solutions (analytical grade solvents from Aldrich). Typically, 1000 scans with 2 cm^{-1} spectral resolution were averaged to optimize the signal-to-noise ratio.

A variable-temperature Specac P/N 21525 cell, with interchangeable pairs of NaCl or quartz windows for transmission spectroscopic studies, was used to record FT-IR spectra at different temperatures. The variable-temperature cell consists of a surrounding vacuum jacket (0.5 Torr), and combines a refrigerant Dewar and a heating block as the sample holder. It is also equipped with a copper-constantan thermocouple for temperature monitoring purposes, and any temperature from -190°C to 250°C (83 – 523 K) can be achieved. Samples were inserted into the heating block part or the Dewar/cell holder assembly in the form of KBr pellets, and infrared spectra were recorded after waiting for thermal equilibration of the sample, which required 20 min for every increment of 10°C . Density functional theory (DFT) calculations were carried out by means of the Gaussian 98 program^[23] running on an SGI Origin 2000 supercomputer. We used Becke's three-parameter exchange functional combined with the LYP correlation functional (B3LYP).^[24] It has previously been shown that for medium-sized molecules the B3LYP functional yields similar geometries as MP2 calculations with the same basis sets.^[25,26] Moreover, the DFT force fields calculated using the B3LYP functional yield infrared spectra in very good agreement with those obtained experimentally.^[27,28] We made use of the 6-31G** basis set.^[29] Molecular geometries were optimized for isolated entities in vacuo. All geometrical parameters were allowed to vary independently, apart from the planarity of the rings. Harmonic vibrational frequencies and infrared and Raman intensities were also calculated analytically for the resulting ground-state optimized geometries with the B3LYP functional.

We applied the often-practiced adjustment of the theoretical force fields in which frequencies are uniformly scaled down by a factor of 0.96, as

recommended by Scott and Radom.^[27] This scaling procedure is often accurate enough to disentangle serious experimental misassignments. All vibrational frequencies quoted herein are thus scaled values. The theoretical spectra were obtained by convoluting the scaled frequencies with Gaussian functions (width-at-half-height 10 cm^{-1}). The relative heights of the Gaussians were determined from the theoretical Raman scattering activities.

Vertical electronic excitation energies were computed by using the time-dependent DFT (TDDFT) approach.^[30,31] At least twelve lowest energy electronic excited states were computed for all the molecules. Previously reported numerical applications have indicated that TDDFT employing current exchange-correlation functionals performs significantly better than HF-based single excitation theories for the low-lying valence excited states of both closed-shell and open-shell molecules.^[32] TDDFT calculations were carried out using the B3LYP functional and the 6-31G** basis set on the previously optimized molecular geometries obtained at the same level of calculation.

Dithieno[3,2-*b*:2',3'-*d*]thiophene-2-carbaldehyde (DTT-A₁): Phosphoryl chloride (1.53 g , $1.0 \times 10^{-2}\text{ mol}$) was added dropwise to a stirred solution of **DTT**^[33] (0.98 g , $5.0 \times 10^{-3}\text{ mol}$) in DMF (15 mL) at 0°C , during which the color changed from pale yellow to yellow with a green tint. Stirring was continued for a further 1 h at 0°C and then the mixture was allowed to warm to room temperature, whereupon yellow crystals precipitated. The resulting suspension was heated to 50°C for 40 min with stirring, and then cooled to room temperature once more. The reaction mixture was poured into ice-chilled water, and saturated sodium acetate solution was added until a pH of around 5 was reached. After storing the mixture in a refrigerator overnight, a dark yellow suspension was obtained, which was filtered. The filtered solid was washed thoroughly with water and then dried, yielding 0.9 g (88%) of the product. The dried product was treated with *n*-hexane, in which the unreacted starting material is completely soluble but not the product. The final yield of the **DTT-A₁** product (spectroscopic data were in accord with those previously described)^[34] was 0.85 g (83%). ^1H NMR (CDCl_3): $\delta = 7.29$ (d, 1H, $J = 4.3\text{ Hz}$), 7.57 (d, 1H, $J = 4.3\text{ Hz}$), 7.97 (s, 1H), 9.96 ppm (s, 1H); EI-MS: m/z (%): 224 ($[M^+]$, 52), 195 (19), 151 (47), 93 (52), 69 (100).

2-[4-(*N,N*-Dibutylamino)styr-1-yl]dithieno[3,2-*b*:2',3'-*d*]thiophene (D₁-DTT): **DTT-A₁** (0.225 g , $1.0 \times 10^{-3}\text{ mol}$) and a catalytic amount of [18]crown-6 were added to a stirred suspension of [4-(*N,N*-dibutylamino)benzyl]triphenylphosphonium iodide^[35] (0.607 g , $1.0 \times 10^{-3}\text{ mol}$) and potassium *tert*-butoxide (0.224 g , $2.0 \times 10^{-3}\text{ mol}$) in dichloromethane (30 mL) at room temperature. The orange suspension changed first to green-orange and then to yellow-green as the solids dissolved. The reaction was nearly complete within 2 h. The reaction mixture was treated with Celite to remove the crown ether, then filtered, and the Celite was washed with fresh solvent. The combined filtrate and washings were concentrated to dryness to leave a greenish-brown residue. The solid mixture was then chromatographed on a silica gel column using dichloromethane as the eluent. A fraction of an orange solution with a green fluorescence was collected, evaporation of the solvent from which left a semi-solid film, which gradually crystallized under ambient conditions. The crystalline solid could be separated by washing away the noncrystalline material with *n*-pentane. The product was obtained as a dark orange solid, 0.179 g (42% yield). ^1H NMR (CDCl_3): $\delta = 0.96$ (t, 6H, $J = 7.3\text{ Hz}$), 1.34 (m, 4H), 1.57 (m, 4H), 3.27 (t, 4H, $J = 7.3\text{ Hz}$), 6.61 (d, 2H, $J = 8.6\text{ Hz}$), 6.83 (d, 1H, $J = 15.8\text{ Hz}$), 7.00 (d, 1H, $J = 15.8\text{ Hz}$), 7.12 (s, 1H), 7.26 – 7.34 (m, 4H); ^{13}C NMR (CDCl_3): $\delta = 14.0, 20.3, 29.5, 50.8, 111.6, 117.2, 117.6, 120.7, 123.7, 125.5, 127.7, 129.0, 140.8, 141.7, 145.3, 148.0$; EI-MS: m/z (%): 425 ($[M^+]$, 100), 382 (70), 340 (70), 325 (50), 296 (50).

2-(Dithieno[3,2-*b*:2',3'-*d*]thiophen-2-ylmethylene)malononitrile (DTT-A₂): In a flask fitted with a Dean-Stark trap, a solution of **DTT-A₁** (8.3 mg , $0.037 \times 10^{-3}\text{ mol}$) and malononitrile (4.9 mg , $0.074 \times 10^{-3}\text{ mol}$) in toluene (25 mL) was heated to reflux for 24 h. A solution of NH_4OAc (1.0 g , $13 \times 10^{-3}\text{ mol}$) in AcOH (3 mL) was then added in portions. After cooling to room temperature, the mixture was diluted with CH_2Cl_2 (50 mL) and washed with water ($3 \times 25\text{ mL}$). The organic layer was dried over MgSO_4 , the solvent was removed to leave a red solid, and this was washed with hexane to obtain the desired product as an orange solid in 90% yield. ^1H NMR (CDCl_3): $\delta = 7.35$ (d, 1H, $J = 5.2\text{ Hz}$), 7.63 (d, 1H, $J = 5.2\text{ Hz}$), 7.84 (s, 1H), 7.94 ppm (s, 1H); ^{13}C NMR (CDCl_3): $\delta =$

60.3, 72.3, 114.1, 114.8, 121.9, 133.5, 134.9, 135.3, 138.9, 142.1, 148.1, 153.6 ppm; EI-MS: m/z (%): 272 ($[M^+]$), 19, 84 (42), 69 (32), 66 (100).

Acknowledgements

S.D.L., R.P.O., M.C.R.D., Y.V., E.P.I., V.H., and J.T.L.N. acknowledge the Dirección General de Enseñanza Superior (DGES, MEC, Spain) and the Junta de Andalucía (Spain) for financial support of the part of this research performed at the University of Málaga through projects BQU2000–1156, BQU2001–1890, and BQU2003–3194, and grants FQM-0159 and FQM-0209. J.C. thanks the Ministerio de Ciencia y Tecnología (MCyT) of Spain for a “Ramón y Cajal” position of chemistry at the University of Málaga. M.C.R.D. and Y.V. are also indebted to the MCyT for their personal fellowships.

- [1] a) A. Slama-Schwok, M. Blanchard-Desce, J.-M. Lehn, *J. Phys. Chem.* **1990**, *94*, 3894; b) M. Barzoukas, M. Blanchard-Desce, D. Josse, J.-M. Lehn, *J. Zyss, Chem. Phys.* **1989**, *133*, 323; c) M. Blanchard-Desce, R. Wortmann, S. Lebus, J.-M. Lehn, P. Krämer, *Chem. Phys. Lett.* **1995**, *243*, 526; d) M. Blanchard-Desce, C. Runser, A. Fort, M. Barzoukas, J.-M. Lehn, V. Bloy, V. Alain, *Chem. Phys.* **1995**, *199*, 253; e) T. Verbiest, S. Houbrechts, M. Kauranen, K. Clays, A. Persoons, *J. Mater. Chem.* **1997**, *7*, 2175.
- [2] F. Würthner, F. Effenberger, R. Wortmann, P. Krämer, *Chem. Phys.* **1993**, *173*, 305.
- [3] I. Cabrera, O. Althoff, H.-T. Man, H. N. Yoon, *Adv. Mater.* **1994**, *6*, 43.
- [4] S. R. Marder, J. W. Perry, B. G. Tiemann, C. G. Gorman, S. Gilmour, S. L. Biddle, G. Bourhill, *J. Am. Chem. Soc.* **1993**, *115*, 2524.
- [5] M. Blanchard-Desce, V. Alain, P. V. Bedworth, S. R. Marder, A. Fort, C. Runser, M. Barzoukas, S. Lebus, R. Wortmann, *Chem. Eur. J.* **1997**, *3*, 1091.
- [6] H. Brisset, C. Thobie-Gautier, M. Jubault, A. Gorgues, J. Roncali, *J. Chem. Soc. Chem. Commun.* **1994**, 1305.
- [7] J. Roncali, C. Thobie-Gautier, *Adv. Mater.* **1994**, *6*, 846.
- [8] S. L. Gilat, S. H. Kawai, J.-M. Lehn, *J. Chem. Soc. Chem. Commun.* **1993**, 1439; S. L. Gilat, S. H. Kawai, J.-M. Lehn, *Chem. Eur. J.* **1995**, *1*, 275; U. Lawrentz, W. Grahn, K. Lukaszk, C. Klein, R. Wortmann, A. Feldner, D. Scherer, *Chem. Eur. J.* **2002**, *8*, 1573.
- [9] Y. Mazaki, K. Kobayashi, *Tetrahedron Lett.* **1989**, *30*, 3315.
- [10] O.-K. Kim, A. Fort, M. Barzoukas, M. Blanchard-Desce, J.-M. Lehn, *J. Mater. Chem.* **1999**, *9*, 2227.
- [11] A. Sakamoto, Y. Furukawa, M. Tasumi, *J. Phys. Chem.* **1994**, *98*, 4635.
- [12] N. Yokonuma, Y. Furukawa, M. Tasumi, M. Kuroda, J. Nakayama, *Chem. Phys. Lett.* **1996**, *255*, 431.
- [13] a) J. Casado, V. Hernandez, S. Hotta, J. T. Lopez Navarrete, *J. Chem. Phys.* **1998**, *109*, 10419; b) C. Moreno Castro, M. C. Ruiz Delgado, V. Hernandez, S. Hotta, J. Casado, J. T. Lopez Navarrete, *J. Chem. Phys.* **2002**, *116*, 10419; c) C. Moreno Castro, M. C. Ruiz Delgado, V. Hernandez, Y. Shirota, J. Casado, J. T. Lopez Navarrete, *J. Phys. Chem. B* **2002**, *106*, 7163; d) J. Casado, R. G. Hicks, V. Hernandez, D. J. T. Myles, M. C. Ruiz Delgado, J. T. Lopez Navarrete, *J. Chem. Phys.* **2003**, *118*, 1912; e) V. Hernandez, S. Hotta, J. T. Lopez Navarrete, *J. Chem. Phys.* **1998**, *109*, 2543.
- [14] a) J. Casado, T. F. Otero, S. Hotta, V. Hernandez, F. J. Ramirez, J. T. Lopez Navarrete, *Opt. Mater. Opt.* **1998**, *9*, 82; b) J. Casado, V. Hernandez, S. Hotta, J. T. Lopez Navarrete, *Adv. Mater.* **1998**, *10*, 1258; c) J. Casado, H. E. Katz, V. Hernandez, J. T. Lopez Navarrete, *J. Phys. Chem. B* **2002**, *106*, 2488; d) J. Casado, L. L. Miller, K. R. Mann, T. M. Pappenfus, V. Hernandez, J. T. Lopez Navarrete, *J. Phys. Chem. B* **2002**, *106*, 3597; e) J. Casado, L. L. Miller, K. R. Mann, T. M. Pappenfus, Y. Kanemitsu, E. Orti, P. M. Viruela, R. Pou-Amerigo, V. Hernandez, J. T. Lopez Navarrete, *J. Phys. Chem. B* **2002**, *106*, 3872; f) J. Casado, M. C. Ruiz Delgado, Y. Shirota, V. Hernandez, J. T. Lopez Navarrete, *J. Phys. Chem. B* **2003**, *107*, 2637; g) J. Casado, L. L. Miller, K. R. Mann, T. M. Pappenfus, H. Higuchi, E. Orti, B. Milian, R. Pou-Amerigo, V. Hernandez, J. T. Lopez Navarrete, *J. Am. Chem. Soc.* **2002**, *124*, 12380.
- [15] a) V. Hernandez, J. Casado, F. Effenberger, J. T. Lopez Navarrete, *J. Chem. Phys.* **2000**, *112*, 5105; b) M. Gonzalez, J. L. Segura, C. Seoane, N. Martin, J. Garin, J. Orduna, R. Alcala, B. Villacampa, V. Hernandez, J. T. Lopez Navarrete, *J. Org. Chem.* **2001**, *66*, 8872.
- [16] a) M. C. Ruiz Delgado, V. Hernandez, J. Casado, J. T. Lopez Navarrete, J.-M. Raimundo, P. Blanchard, J. Roncali, *Chem. Eur. J.* **2003**, *9*, 3670; b) J. Casado, T. M. Pappenfus, L. L. Miller, K. R. Mann, T. M. Pappenfus, E. Orti, P. M. Viruela, R. Pou-Amerigo, V. Hernandez, J. T. Lopez Navarrete, *J. Am. Chem. Soc.* **2003**, *125*, 2534; A. Abbotto, L. Beverina, S. Bradamante, A. Facchetti, C. Klein, G. A. Pagani, M. Redi-Abshiro, R. Wortmann, *Chem. Eur. J.* **2003**, *9*, 1991.
- [17] a) G. Zerbi, C. Castiglioni, M. Del Zoppo, *Electronic Materials: The Oligomer Approach*, Wiley-VCH, Weinheim, **1998**, p. 345; b) C. Castiglioni, M. Gussoni, J. T. Lopez Navarrete, G. Zerbi, *Solid State Commun.* **1988**, *65*, 625; c) J. T. Lopez Navarrete, G. Zerbi, *J. Chem. Phys.* **1991**, *94*, 957 and 965; d) V. Hernandez, C. Castiglioni, M. Del Zoppo, G. Zerbi, *Phys. Rev. B* **1994**, *50*, 9815; e) E. Agosti, M. Rivola, V. Hernandez, M. Del Zoppo, G. Zerbi, *Synth. Met.* **1999**, *100*, 101.
- [18] a) Ch. Ehrendorfer, A. Karpfen, *J. Phys. Chem.* **1994**, *98*, 7492; b) Ch. Ehrendorfer, A. Karpfen, *J. Phys. Chem.* **1995**, *99*, 5341.
- [19] F. Effenberger, F. Würthner, F. Steybe, *J. Org. Chem.* **1995**, *60*, 2082.
- [20] F. J. Ramirez, M. A. G. Aranda, V. Hernandez, J. Casado, S. Hotta, J. T. Lopez Navarrete, *J. Chem. Phys.* **1998**, *109*, 1920.
- [21] Y. Shirota, *J. Mater. Chem.* **2000**, *10*, 1.
- [22] U. Mitschke, P. Bäuerle, *J. Mater. Chem.* **2000**, *10*, 1471.
- [23] M. J. Frisch, G. W. Trucks, H. B. Schlegel, G. E. Scuseria, M. A. Robb, J. R. Cheeseman, V. G. Zakrzewski, J. A. Montgomery, R. E. Stratman, S. Burant, J. M. Dapprich, J. M. Millam, A. D. Daniels, K. N. Kudin, M. C. Strain, O. Farkas, J. Tomasi, V. Barone, M. Cossi, R. Cammi, B. Mennucci, C. Pomelli, C. Adamo, S. Clifford, G. Ochterski, A. Petersson, P. Y. Ayala, Q. Cui, K. Morokuma, D. K. Malick, A. D. Rabuck, K. Raghavachari, J. B. Foresman, J. Cioslowski, J. V. Ortiz, B. B. Stefanov, G. Liu, A. Liashenko, I. Piskorz, I. Komaromi, R. Gomperts, R. L. Martin, D. J. Fox, T. Keith, M. A. Al-Laham, C. Y. Peng, A. Nanayakkara, C. Gonzalez, M. Challacombe, P. M. W. Gill, B. G. Johnson, W. Chen, M. W. Wong, J. L. Andres, M. Head-Gordon, E. S. Replogle, J. A. Pople, *Gaussian 98, Revision A.7*, Gaussian Inc., Pittsburgh PA, **1998**.
- [24] A. D. Becke, *J. Chem. Phys.* **1993**, *98*, 1372.
- [25] P. J. Stephens, F. J. Devlin, F. C. F. Chabalowski, M. J. Frisch, *J. Phys. Chem.* **1994**, *98*, 11623.
- [26] J. J. Novoa, C. Sosa, *J. Phys. Chem.* **1995**, *99*, 15837.
- [27] A. P. Scott, L. Radom, *J. Phys. Chem.* **1996**, *100*, 16502.
- [28] G. Rauhut, P. Pulay, *J. Phys. Chem.* **1995**, *99*, 3093.
- [29] M. M. Francl, W. J. Pietro, W. J. Hehre, J. S. Binkley, M. S. Gordon, D. J. Defrees, J. A. Pople, *J. Chem. Phys.* **1982**, *77*, 3654.
- [30] a) E. Runge, E. K. U. Gross, *Phys. Rev. Lett.* **1984**, *52*, 997; b) E. K. U. Gross, W. Kohn, *Adv. Quantum Chem.* **1990**, *21*, 255; c) *Density Functional Theory: Proceedings of the NATO Advanced Study Institute* (Eds.: E. K. U. Gross, R. M. Dreizler), Plenum Press, New York, **1995**, p. 149.
- [31] M. E. Casida, in *Recent Advances in Density Functional Methods, Part I* (Ed.: D. P. Chong), World Scientific, Singapore, **1995**, p. 115.
- [32] W. Koch, M. C. Holthausen, *A Chemist's Guide to Density Functional Theory*, Wiley-VCH, Weinheim, **2000**.
- [33] F. De Jong, M. J. Janssen, *J. Org. Chem.* **1971**, *36*, 1645.
- [34] G. Kossmehl, P. Beimling, G. Manecke, *Makromol. Chem.* **1982**, *183*, 2771–2786.
- [35] H. Bredereck, G. Simchen, W. Griebenow, *Chem. Ber.* **1973**, *106*, 3732.

Received: November 27, 2003
 Revised: February 16, 2004
 Published online: June 21, 2004